WebLog Journal of Materials Science and Engineering

Research Article
Published: 30 Jun, 2026

Morphological Persistence from SEM: Threshold–Fractal Signatures with Occupancy-Controlled Binarization

Helena Cristina Vasconcelos[1,2] and Maria Gabriela Meirelles[1,3]*

[1]Faculty of Sciences and Technology, University of the Azores, Ponta Delgada, S. Miguel, 9500-321 Azores, Portugal

[2]Laboratory of Instrumentation, Biomedical Engineering and Radiation Physics (LIBPhys, UNL), Department of Physics, NOVA School of Science and Technology, 2829-516 Caparica, Portugal

[3]Research Institute of Marine Sciences of the University of the Azores (OKEANOS), Horta, Faial, 9901-862 Azores, Portugal

WebLog Open Access Publications
Article ID : wjmse.2026.f3005
Author : Helena Cristina Vasconcelos

OPEN ACCESS

Correspondence:
Helena Cristina Vasconcelos, Faculty of Sciences and Technology, University of the Azores, Ponta Delgada, S. Miguel, 9500-321 Azores, Portugal, Tel: 296650000;
E-mail: helena.cs.vasconcelos@uac.pt
ORCID: https://orcid.org/0000-0001-5935-870X

Received Date: *07 Jun 2026*
Accepted Date: *29 Jun 2026*
Published Date: *30 Jun 2026*

Citation:
Vasconcelos HC, Meirelles MG. Morphological Persistence from SEM: Threshold–Fractal Signatures with Occupancy-Controlled Binarization. WebLog J Materials Sci Eng. wjmse.2026.f3005. https://doi.org/10.5281/zenodo.21431094

Abstract

Scanning electron microscopy (SEM) micrographs are routinely interpreted qualitatively, yet they encode reproducible lateral morphology patterns that can be quantified without invoking height metrology. Here we propose a compact, practical protocol to extract a morphological persistence signature from SEM intensity fields using threshold-dependent box-counting fractal analysis with explicit preprocessing-sensitivity checks. We show that fixed normalized thresholds can fail for certain microstructures by driving the binary representation into a low-support regime at high thresholds, rendering the excursion sets visually uninformative and fractal estimates unstable. To address this failure mode, we introduce occupancy-controlled (percentile-based) thresholding that enforces comparable foreground occupancy across the threshold series, enabling meaningful multiscale comparison. Applying this protocol to two contrasting SEM textures (grain-like and agglomerate-like), we report threshold-dependent fractal dimensions *Df(T)* and quantify sensitivity to three standard preprocessing strategies (linear rescaling, histogram equalization, and CLAHE). The resulting persistence profiles provide a reproducible SEM-only criterion to compare microstructures and to flag when apparent "fractal complexity" is dominated by segmentation sensitivity rather than persistent image-field morphology.

Keywords: SEM; Image Analysis; Box-counting; Fractal Dimension; Thresholding; Preprocessing Sensitivity; Microstructure; Morphological Persistence

Introduction

Scanning electron microscopy (SEM) is a central tool for microstructure assessment across materials science, yet quantitative descriptors extracted from SEM images often remain sensitive to segmentation and contrast choices. A key reason is that SEM grayscale intensity is generally not a metrically calibrated height field: secondary-electron contrast depends on edge/orientation effects, detector geometry, and, when present, charging or compositional contributions. Consequently, SEM intensity maps are more reliably treated as two-dimensional scalar morphology fields for comparative analysis rather than direct topography proxies—an issue closely connected to broader nanometrology challenges of resolution, stochasticity, and image-based inference [1].

Building on this SEM-as-field viewpoint, the authors recently demonstrated that single SEM micrographs can support multiscale descriptors combining PSD/H, multifractal spectra $f(\alpha)$, lacunarity, and Minkowski/Euler functionals to characterize intermittency, heterogeneity, and connectivity in thin-film morphology [2]. In parallel, threshold-dependent box-counting fractal analysis has been applied to sputtered TiO_2 thin films by scanning multiple thresholds $T = \{0.50, 0.60, 0.70, 0.75, 0.80\}$ and combining D_f with texture statistics, such as GLCM, to reduce dependence on a single segmentation level [3]. This direction aligns with continued interest in fractal descriptors for thin-film topography and microstructure comparison, as surveyed in recent thin-film fractal reviews [4], and with broader materials-processing studies where SEM is used as a primary morphological probe alongside structural characterization [5].

At the same time, image-based morphology quantification benefits from principled geometric and statistical frameworks. Integral-geometry morphological image analysis provides a rigorous route to real-space characterization of spatial patterns and motivates reporting not only a single descriptor but families of descriptors that respond predictably to scale and thresholding [6]. Within this framework, Minkowski functionals and related morphological descriptors provide a statistical-physics basis for quantifying spatial organization, connectivity, and topology changes in thresholded fields [7]. Together, these foundations clarify a practical point that is often underreported in SEM-fractal workflows: threshold choice is part of the analysis protocol, not a neutral preprocessing detail.

A concrete failure mode follows. Fixed normalized thresholds can drive the binarized excursion set into a low-support regime, where the foreground becomes sparse and visually uninformative. In that regime, box-counting slopes become dominated by loss of structural support, preprocessing sensitivity, and finite-size effects, and the inferred "fractal complexity" may reflect segmentation-induced support loss rather than persistent image-field morphology. The goal of the present work is therefore methodological and diagnostic: we (i) quantify threshold-induced support loss via an occupancy curve $\varphi(T)$, defined as the foreground fraction versus threshold; (ii) introduce occupancy-controlled percentile-based thresholding as a minimal remedy when fixed thresholds produce low foreground support; and (iii) quantify preprocessing sensitivity under standard image-normalization strategies: linear rescaling, histogram equalization, and CLAHE. The intended output is not a single absolute fractal number, but a morphological persistence profile—how inferred structure survives thresholding and preprocessing—providing an SEM-only criterion to compare microstructures while remaining consistent with the SEM-field framework [1–4, 6].

The protocol is demonstrated on two contrasting SEM textures, chosen to represent markedly different morphological organizations. Representative input micrographs are drawn from prior microstructure studies on hydroxyapatite/zirconia composites, where SEM was used to document dense grain-scale microstructures and agglomerated nanoscale textures [8]. We emphasize that the novelty here lies in the analysis workflow and diagnostics—occupancy-based low-support detection, occupancy-controlled thresholding, and preprocessing-sensitivity reporting—rather than in the acquisition of new SEM images.

Materials and Methods

SEM images and region of interest (ROI)

Two representative SEM micrographs, hereafter referred to as SEM A and SEM B, were analyzed as 2D grayscale morphology fields. The SEM inputs were drawn from prior microstructure studies on hydroxyapatite/zirconia composites, where SEM was used to document dense grain-scale and agglomerated nanoscale textures [8]. Each image was cropped to remove borders and annotation regions, retaining a high-texture ROI. The analysis is comparative and does not interpret SEM intensity as metrically calibrated height, consistent with SEM-based nanometrology constraints [1].

Intensity normalization and preprocessing sensitivity

1. Each ROI was mapped to a normalized intensity field $I(x,y) \in [0,1]$. To quantify sensitivity to standard contrast-normalization choices, the full workflow was repeated under three preprocessing strategies:Linear rescaling (global contrast stretching using a fixed percentile range),

2. Global histogram equalization,

3. CLAHE (contrast-limited adaptive histogram equalization; fixed clip limit).

This preprocessing-sensitivity analysis follows the general principle that SEM-derived descriptors should be tested against reasonable image-normalization perturbations [1–4].

Thresholding strategies and excursion sets

Binary excursion sets were defined as:

$M_T = \{(x,y): I(x,y) \geq T\}$

A mild binary cleaning step (removal of very small objects and holes) was applied to suppress isolated pixel artifacts.

Two thresholding strategies were used:

1. Fixed-threshold series, applied to SEM B: $T = \{0.50, 0.60, 0.70, 0.75, 0.80\}$,

consistent with the multi-threshold practice adopted in previous fractal-SEM work [3] and with thin-film fractal workflows surveyed in the literature [4].

2. Occupancy-controlled percentile-based series, applied to SEM A: thresholds were selected to target a controlled sequence of foreground occupancies, approximately 35%, 25%, 15%, 10%, and 6%. This avoids loss of structural support when fixed thresholds become too selective for a given intensity distribution, as discussed in Section 3.1.

Occupancy diagnostic and low-support criterion

Foreground occupancy was defined as:

$\phi(T) = \frac{|M_T|}{|\Omega|}$,

the fraction of ROI pixels above the threshold. We define a practical low-support regime when $\phi(T) \lesssim 5\%$, where the binary support becomes too sparse for visually and statistically meaningful multiscale characterization. This value is used as an operational warning threshold, not as a universal physical transition. It operationalizes the broader warning that box-counting estimates are sensitive to support definition and finite-size effects [4, 6].

Box-counting fractal dimension

For each binary map M_T, the box-counting number $N(\ell)$ was computed using non-overlapping square boxes of side ℓ, with ℓ taken as powers of two in pixel units. Boxes containing at least one foreground pixel were counted. The box-counting fractal dimension was estimated from the log–log slope over intermediate scales:

$$D_f(T) = \frac{d\log N(\ell)}{d\log (1/\ell)}.$$

To reduce saturation and edge effects, the smallest and largest box sizes were excluded when needed, and the fit was restricted to a mid-range scale window, consistent with best-practice cautions in box-counting implementations [4, 6].

Reporting: morphological persistence profiles

Rather than emphasizing a single absolute D_f, we report:

(i) occupancy curves $\varphi(T)$ (low-support diagnostic),

(ii) threshold-dependent $D_f(T)$,

(iii) variability across preprocessing (mean ± standard deviation).

This defines the morphological persistence profile, understood here as the joint response of occupancy, fractal dimension, and preprocessing sensitivity across a threshold series, consistent with the

SEM-field analysis framework [2–4].

Results

Representative SEM inputs

Figure 1 shows the representative SEM inputs analyzed in this work. SEM A exhibits a grain-like texture, whereas SEM B displays an agglomerate-like texture. These two fields are intentionally contrasted to test how threshold–fractal workflows behave under markedly different intensity distributions and morphological organizations.

Fixed-threshold binarization can produce a low-support regime in SEM A

We first assessed whether a fixed-threshold series produced excursion sets with sufficient structural support for meaningful multiscale counting. This was quantified using the occupancy curve $\varphi(T)$, defined as the fraction of pixels above threshold after mild binary cleaning. For SEM A, $\varphi(T)$ decreases sharply as T increases and approaches a low-support regime near $T \gtrsim 0.70$, depending on preprocessing. In this regime, binarized maps become sparse and visually uninformative, and box-counting estimates become increasingly sensitive to finite-size effects and implementation details. By contrast, SEM B maintains substantially higher occupancy across the same threshold range, preserving visible structural support. Importantly, this qualitative difference persists across the three preprocessing strategies, indicating that the low-support response in SEM A is not caused by a single preprocessing choice but reflects the threshold sensitivity of that SEM intensity field (Figure 2).

Threshold series used for box-counting: fixed in SEM B, occupancy-controlled in SEM A

The occupancy diagnostic motivates different threshold parameterizations for the two textures. Because fixed thresholds can drive SEM A toward very low foreground support at higher T, SEM A was analyzed using occupancy-controlled percentile-based thresholds, which enforce a controlled decrease in occupancy while still scanning selectivity systematically. SEM B, in contrast, remains outside the low-support regime under the fixed series $T = \{0.50, 0.60, 0.70, 0.75, 0.80\}$, so fixed-threshold binarization is appropriate there. This combined strategy ensures interpretable excursion sets for multiscale counting in SEM A while preserving a conventional fixed-threshold series for SEM B.

Preprocessing sensitivity of $D_f(T)$

We next evaluated how sensitive the inferred fractal descriptor is to standard preprocessing. Figure 3 reports $D_f(T)$ under linear rescaling, histogram equalization, and CLAHE, together with mean ± standard deviation bands. SEM B exhibits comparatively stable $D_f(T)$ across preprocessing choices, consistent with its well-populated binary support across thresholds. SEM A shows larger variability, consistent with its stronger threshold sensitivity under fixed-threshold parameterization (Section 3.2). These results support the central methodological point of the paper: reporting D_f without occupancy diagnostics and without preprocessing-sensitivity bands can be misleading, because apparent "fractal complexity" may be dominated by segmentation-induced loss of foreground support rather than persistent image-field morphology.

Operational reference at $T = 0.70$

For a compact numerical comparison, we use $T = 0.70$ as an operational reference level because it lies near the onset of the low-support regime for SEM A under fixed thresholding, as diagnosed by $\varphi(T)$ (Figure 2). Table 1 reports D_f at $T = 0.70$ as mean ± standard deviation across preprocessing, together with the min–max range. We emphasize, however, that interpretation relies on the full persistence profiles, namely $\varphi(T)$ and $D_f(T)$ considered together, rather than on a single-threshold value.

Discussion

A central methodological message of this work is that threshold selection is part of the analysis protocol when fractal descriptors are extracted from SEM intensity fields. SEM grayscale is not height-calibrated and may exhibit strongly non-uniform intensity distributions; therefore, fixed normalized thresholds do not necessarily correspond to comparable segmentation levels across distinct textures or even across preprocessing choices [1, 4]. This is not a minor technicality: once the binary excursion set becomes too sparse, box-counting estimates are no longer controlled primarily by multiscale structure but by loss of foreground support and finite-size effects [4, 6].

Occupancy as the missing diagnostic in SEM threshold–fractal workflows

Threshold-dependent fractal analysis is routinely used to summarize multiscale complexity from binarized images, but SEM intensity fields are particularly prone to threshold sensitivity because they are not height-calibrated and can exhibit strongly non-uniform intensity distributions, including edge effects, orientation contrast, and detector bias. In this setting, a fixed normalized threshold T is

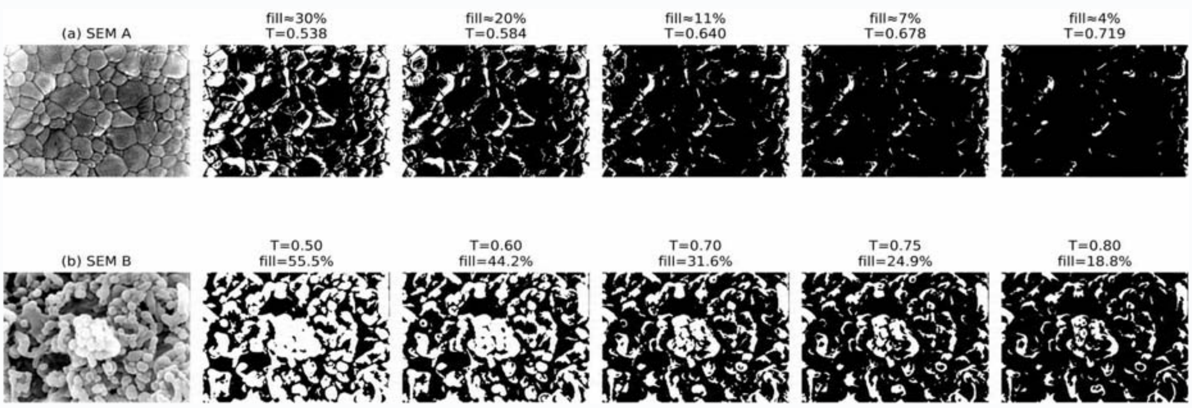

Figure 1: Representative SEM inputs and corresponding thresholded excursion sets used for the analysis: (a) SEM A (grain-like texture) using occupancy-controlled thresholds and (b) SEM B (agglomerate-like texture) using fixed thresholds.

Table 1: Diagnostic operational-threshold summary at T = 0.70: mean fractal dimension $\bar{D_f}$, preprocessing sensitivity $s(D_f)$, min–max range, and $\bar{D_f} \pm s(D_f)$.

SEM	T	$\bar{D_f}$	$s(D_f)$	D_f^{min}	D_f^{max}	$\bar{D_f} \pm s(D_f)$
SEM A	0.70	1.035	0.603	0.400	1.599	1.035 ± 0.603
SEM B	0.70	1.527	0.156	1.351	1.647	1.527 ± 0.156

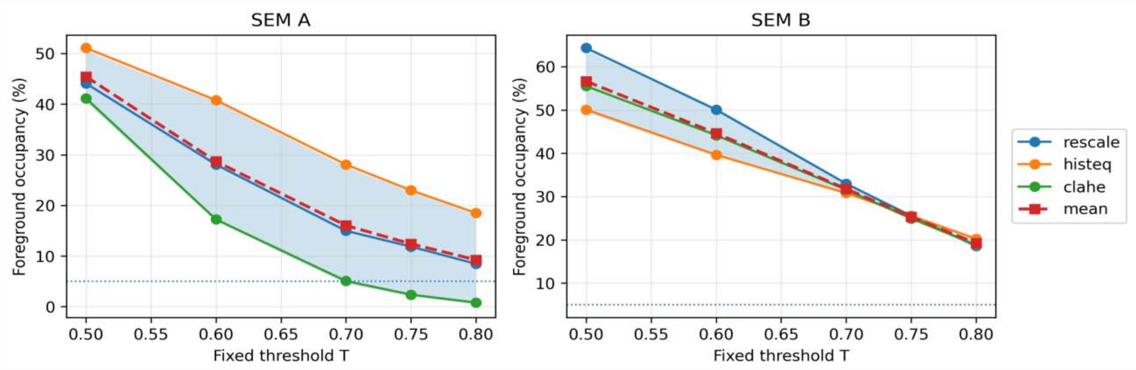

Figure 2: Occupancy response under fixed-threshold binarization: foreground occupancy *φ(T)* versus threshold *T*. The dotted line marks the approximately 5% practical low-support warning level.

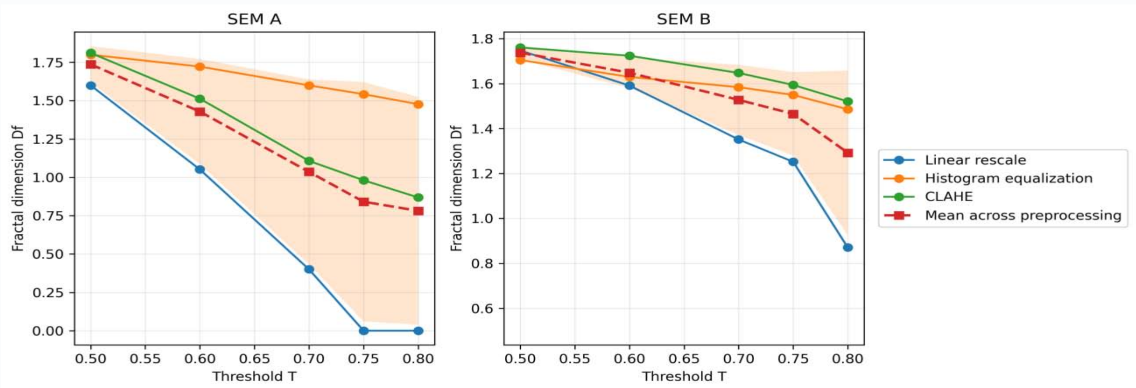

Figure 3: Threshold-dependent fractal dimension $D_f(T)$ obtained under different preprocessing strategies. Shaded regions represent preprocessing-induced variability.

not a physically invariant parameter; it is a segmentation rule whose outcome depends on the image histogram and on preprocessing. The occupancy curve *φ(T)* therefore provides a minimal and transparent diagnostic of whether a chosen threshold series remains in a regime where excursion sets carry enough structural support for multiscale characterization.

Our results show that SEM A approaches a low-support regime near $T \approx 0.70$ under fixed thresholding, whereas SEM B remains well above this regime across the same threshold range (Figure 2). Importantly, this conclusion is consistent across three standard preprocessing strategies. This supports a key methodological point: without reporting *φ(T)*, a threshold–fractal analysis can unintentionally operate in a low-support regime, where $D_f(T)$ reflects loss of structural support and finite-size artifacts rather than persistent morphology in the SEM intensity field.

Morphological persistence as the interpretable output, not a single "fractal number"

A common pitfall in SEM-based fractal analysis is to interpret D_f as an absolute property of the sample. In a 2D SEM-field framework, a more defensible interpretation is comparative and procedural: $D_f(T)$ is a descriptor of how space-filling the binary support is at a given segmentation level, while the pair $\{D_f(T), \varphi(T)\}$ across thresholds quantifies how structure persists as segmentation becomes more selective. This motivates the concept of a morphological persistence profile: the joint behavior of (i) occupancy *φ(T)*, (ii) threshold-dependent $D_f(T)$, and (iii) preprocessing sensitivity under controlled image-normalization choices. In this view, SEM B exhibits a more persistent threshold-dependent morphology: its supports remain well populated and its $D_f(T)$ is less sensitive to preprocessing. SEM A, by contrast, is threshold-fragile under fixed thresholds, meaning that a fixed-threshold series can quickly eliminate structural support and drive $D_f(T)$ into an unstable regime. This distinction remains informative even when the absolute intensity-to-height mapping is undefined: it characterizes lateral organization and segmentation stability, not topographic metrology.

Why occupancy-controlled thresholding is a legitimate remedy and when it should be used

When fixed thresholds drive the binary support into a low-occupancy regime, the methodological choice is not between fixed

Table 2: Minimal reporting checklist for threshold–fractal SEM workflows.

Item	What to report	Why it matters
Occupancy diagnostic	$\varphi(T)$, or fill percentage, for each threshold in the series	Detects low-support regimes; without it, D_f may reflect foreground loss rather than structure
Low-support flag	Mark thresholds where $\varphi(T) \lesssim 5\%$	Avoids interpreting $D_f(T)$ in a poorly populated binary-support regime
Threshold strategy	Fixed-T or occupancy-controlled percentile thresholding, with the chosen schedule	Makes the segmentation level explicit and reproducible
Preprocessing sensitivity	$D_f(T)$ under at least three preprocessing strategies, with mean ± standard deviation band	Separates persistent image-field morphology from preprocessing artifacts
Fit window disclosure	Box sizes used and mid-range fit window, excluding extremes when needed	Controls known box-counting sensitivities
Interpretation boundary	State explicitly: "SEM-field descriptor, not height metrology"	Prevents over-claiming physical roughness exponents

and arbitrary threshold selection; it is between (a) operating in a demonstrably low-support regime or (b) adopting a threshold parameterization that preserves interpretable supports while still scanning selectivity systematically. Occupancy-controlled percentile-based thresholding does precisely that: it replaces "threshold as an absolute intensity level" with "threshold as a controlled occupancy level", ensuring that the excursion set remains sufficiently populated for multiscale counting. In SEM A, occupancy-controlled thresholds provide an interpretable threshold series by enforcing a controlled decrease in occupancy, from approximately 30% down to 4–6%, which keeps the binary supports visible and statistically usable. In SEM B, fixed thresholds already produce well-populated binary supports, so occupancy control is optional rather than necessary. The combined strategy adopted here—occupancy control when fixed thresholds lead to low support; fixed thresholds when they do not—provides a pragmatic and reproducible workflow.

Generalization, limitations, and what this does not claim

The present protocol is intentionally minimal and SEM-only. It does not claim calibrated roughness or height exponents; it treats SEM intensity as a 2D morphology field. It also does not claim universality of any particular threshold set. Rather, it provides a diagnostic and a decision rule: if fixed thresholds lead to loss of foreground support, occupancy-controlled thresholding should be used. This rule can be applied to other SEM datasets.

Limitations include: (i) a representative-image demonstration per texture type; (ii) dependence of D_f on ROI selection; and (iii) finite-size effects in box-counting fits. These are precisely why the protocol emphasizes reporting the occupancy diagnostic (Figure 2) and preprocessing-sensitivity bands (Figure 3). In future applications, statistical strengthening is straightforward: multiple ROIs per sample can be analyzed, distributions of persistence profiles can be reported, and, when available, persistence changes can be related to processing variables or independent measurements.

To prevent common misinterpretations of threshold–fractal SEM workflows, we propose the minimal reporting checklist in Table 2. This is not an "extra step"; it follows directly from the low-support behavior quantified by occupancy (Figure 2) and from the preprocessing-sensitivity bands (Figure 3).

Conclusions

We presented a compact SEM-only protocol that turns threshold–fractal analysis into a reproducible morphological persistence workflow by adding two often overlooked elements: an explicit occupancy diagnostic $\varphi(T)$ and preprocessing-sensitivity assessment. Fixed thresholds may drive certain SEM textures into a low-support regime, producing visually uninformative binary maps and unstable multiscale estimates; this failure mode is detected directly by $\varphi(T)$ (Figure 2) and mitigated using occupancy-controlled percentile-based thresholding. The resulting persistence profiles—jointly reporting $\varphi(T)$ and $D_f(T)$ with preprocessing-induced variability (Figure 3, Table 1)—provide a practical criterion to compare microstructures and to distinguish persistent image-field morphology from segmentation-driven artifacts, supported by a minimal reporting checklist (Table 2).

References

1. Kondi A, Papia E-M, Stai E & Constantoudis V. Computational methods in nanometrology: The challenges of resolution and stochasticity. *Frontiers in Nanotechnology, 2025, 7*, 1559523. https://doi.org/10.3389/fnano.2025.1559523

2. Vasconcelos H. C, Eleutério T, Meirelles M & Özmenteş R. When a surface becomes a network: SEM reveals hidden scaling laws and a percolation-like transition in thin films. *Surfaces, 2026, 9*, 14. https://doi.org/10.3390/surfaces9010014

3. Vasconcelos H. C, Eleutério T & Meirelles M. Surface roughness and fractal analysis of TiO_2 thin films by DC sputtering. *Engineering Proceedings, 2025, 105*, 2. https://doi.org/10.3390/engproc2025105002

4. Zhou W, Cao Y, Zhao H, Li Z, Feng P & Feng F. Fractal analysis on surface topography of thin films: A review. *Fractal and Fractional, 2022, 6*(3), 135. https://doi.org/10.3390/fractalfract6030135

5. Eleutério T, Sério S & Vasconcelos H. C. Growth of nanostructured TiO_2 thin films onto lignocellulosic fibers through reactive DC magnetron sputtering: A XRD and SEM study. *Coatings, 2023, 13*(5), 922. https://doi.org/10.3390/coatings13050922

6. Michielsen K & De Raedt H. Integral-geometry morphological image analysis. *Physics Reports, 2001, 347*(6), 461–538. https://doi.org/10.1016/S0370-1573(00)00106-X

7. Mecke K. R. Additivity, convexity, and beyond: Applications of Minkowski functionals in statistical physics. In K. R. Mecke & D. Stoyan (Eds.), Statistical Physics and Spatial Statistics: The Art of Analyzing and Modeling Spatial Structures and Pattern Formation (Lecture Notes in Physics, 2000, Vol. 554, pp. 111–184). Springer. https://doi.org/10.1007/3-540-45043-2_6

8. Vasconcelos H. C & Barreto M. C. Tailoring the microstructure of sol–gel derived hydroxyapatite/zirconia nanocrystalline composites. *Nanoscale Research Letters, 2011, 6*, 20. https://doi.org/10.1007/s11671-010-9766-z